Remote Sensing Based Water Productivity Assessment –Karaghandy, Kazakhstan

FINAL REPORT

IWMI International Water Management Institute

CGIAR RESEARCH PROGRAM ON Water, Land and Ecosystems

ADB ASIAN DEVELOPMENT BANK

Final Project Report submitted to ADB under the program for Expanding Support to Water Accounting in River Basins and Water Productivity in Irrigation Schemes.

Citation: Khan, A., and Rebelo, L-M., 2020. Remote Sensing Based Water Productivity Assessment: Final Project Report, Karaghandy, Kazakhstan; IWMI, Colombo, Sri Lanka

Cover image: Rural Landscape, Madeline Dahm / IWMI

EXPANDING SUPPORT TO WATER ACCOUNTING IN RIVER BASINS AND WATER PRODUCTIVITY IN IRRIGATION SCHEMES

Project final report:

Remote Sensing Based Water Productivity Assessment, Karaghandy, Kazakhstan

PREPARED FOR THE
ASIAN DEVELOPMENT BANK
BY

The International Water Management Institute

November 2020

TABLE OF CONTENTS

LIST OF FIGURES

LIST OF TABLES

LIST OF ABBREVIATIONS

ADB	Asian Development Bank
AGBP	Above Ground Biomass Production
CWP	Crop Water Productivity
CWSI	Crop Water Stress Index
DSS	Decision Support System
ETa	Actual Evapotranspiration
FAO	Food and Agriculture Organization
GEE	Google Earth Engine
GLDAS	Global Land Data Assimilation System
HI	Harvest Index
IHE Delft	IHE Delft Institute for Water Education
IWMI	International Water Management Institute
IWPIP	Integrated Water Productivity Improvement Project
MODIS	Moderate Resolution Imaging Spectroradiometer
NASA	National Aeronautics and Space Administration
NDVI	Normalized difference vegetation index
pySEBAL	Python implementation of SEBAL
RWD	Relative Water Deficit
SRTM	Shuttle Radar Topography Mission
TA	Technical Assistance
WP	Water Productivity
USGS	United States Geological Survey

I. INTRODUCTION

1. The ADB is committed under its Water Operational Plan 2011-2020 to undertake expanded and enhanced analytical work to enable its developing member countries to secure deeper and sharper understanding of water issues and solutions. IHE Delft, in collaboration with IWMI and FAO, will support ADB in achieving this objective.

2. The activities proposed under the current study build on the work previously undertaken by IHE Delft and IWMI in cooperation with the Asian Development Bank (ADB) to assess crop water productivity and to assess water resource status in selected countries in Asia. Through the current study, IHE Delft in partnership with its subcontracted partner, IWMI, will support (a) ADB's lending and non-lending assistance in the water sector, and (b) the design of irrigation projects at an early stage at selected candidate projects.

3. IHE Delft and IWMI and aim to support ADB's lending and non-lending assistance in the water sector by creating (i) comprehensive, (ii) comprehensible, and (iii) accessible information on available water resources and their current uses in major river basins. IHE Delft and IWMI aim to support the design of, or investments in irrigation schemes at project start by (i) providing baseline data for parameters related to land and water productivity, and (ii) identifying suitable interventions.

4. Assistance is being provided to Projects in 7 countries. The nature of the support provided in each is determined through close consultation with ADB Project Officers, and tailored to the project requirements. In some locations, this may take the form of water accounting assessments to characterize water use and availability, while in others emphasis may be place on water productivity (either crop or biomass water productivity), or on irrigation performance assessments, to target investments.

5. This document is the Final Report for the Kazakhstan case study, and as such it details the activities undertaken by IWMI to undertake Water Productivity analyses in the Karaghandy region of Kazakhstan.

II. PROJECT BACKGROUND

6. The activities reported here are intended to support the proposed Irrigation Rehabilitation Sector Project which is being prepared as part of Kazakhstan Government's "State Program on Development of Agricultural Industry for 2017-2021". The proposed project to be financed under ADB loan stipulates rehabilitation and modernization of agricultural irrigation infrastructure in order to return into operation currently unused 171,100 ha of previously irrigated agricultural lands in East-Kazakhstan, Kyzylorda, Karaghandy, and Zhambyl provinces.

7. During the Soviet period Kazakhstan witnessed extensive, centrally planned irrigation systems that were locally managed and operated. After independence in 1991,

many of these systems fell into a state of disrepair. An ambitious target to rehabilitate 600,000 ha of irrigation systems by 2021 has been set to meet the economic development agenda. To meet this target, the Ministry of Agriculture has initiated a large series of irrigation investment projects for support from international financial institutions, which largely consist of rehabilitation of former irrigation schemes that were plagued by problems and abandoned.

8. In Karaghandy province ADB initially aimed to support rehabilitation of 6 canals and 23 pipelines in 10 schemes of 6 districts, namely Abay, Zhezkazgan, Zhanaarka, Bukhar-Zhyrau (hereafter referred as Bukhar), Osakarovka and Nura districts. The objective would be to support the rehabilitation and improvement of irrigation networks and promote the diversification from traditional low-yielding and low-value grain crops into high-value cash crops. The project was postponed due to delays in processing, however the water productivity studies may still provide valuable information for irrigation rehabilitation and modernization.

III. SCOPE OF SERVICES

9. Through discussions with ADB, IWMI and IHE Delft, it was agreed that the ADB program to support Water Accounting in River Basins and Water Productivity in Irrigation Schemes would be used to characterize the status of water use and availability within irrigated areas, to support the selection of sub projects for investment.

10. To this end, IWMI has undertaken a remote sensing based assessment to provide the information needed for this purpose. This has focused on the analysis of evapotranspiration and water deficits for the northern part of the Karaghandy region where six of the subprojects are located, partially covering the districts of Abay, Zhanaarka, Bukhar, Osakarovka and Nura. The purpose of the activity was to provide an overview of the water productivity situation in the agricultural areas of the province over a single irrigation season, rather than to focus on an individual irrigation scheme in detail and over multiple seasons.

11. IHE Delft and IWMI have proposed to use the pySEBAL approach (detailed in IHE Delft and IWMI, 2020) for analyses at the irrigation command scale to derive the data on Above Ground Biomass Production (AGBP) and the actual Evapotranspiration (ET_a); this approach uses satellite images and weather data as inputs. PySEBAL processes the surface energy balance and plant growth at landscape level with a grid of 30 m independent of crop type information. The ET_a and AGBP can be estimated without any a priori information on the type of crop and type of soil. This approach, and the pySEBAL tool in particular, have been developed through, and widely used in other similar studies funded by ADB and implemented by IHE Delft and IWMI.

12. IWMI performed a water productivity assessment for the irrigation systems identified in order to characterize the water consumed and to identify water related deficits within the Subprojects over a single annual irrigation season, May to October of 2019. The

analysis was performed over a large spatial scale, and included the majority of the cropland area in the Karaghandy province.

13. Six Subprojects to be rehabilitated are located in Karaghandy, covering an area of 27,900 ha. The exact locations of these are not available; however, their approximate locations within the Karaghandy province are indicated in the Report detailing the “Initial Environmental Examination of Subprojects” in Karaghandy Province (IEE, 2019) and indicated in the red circle in Figure 1. From this it is clear that the majority of the irrigation systems are located within the central, northern part of the province. The study has thus focused on this region.

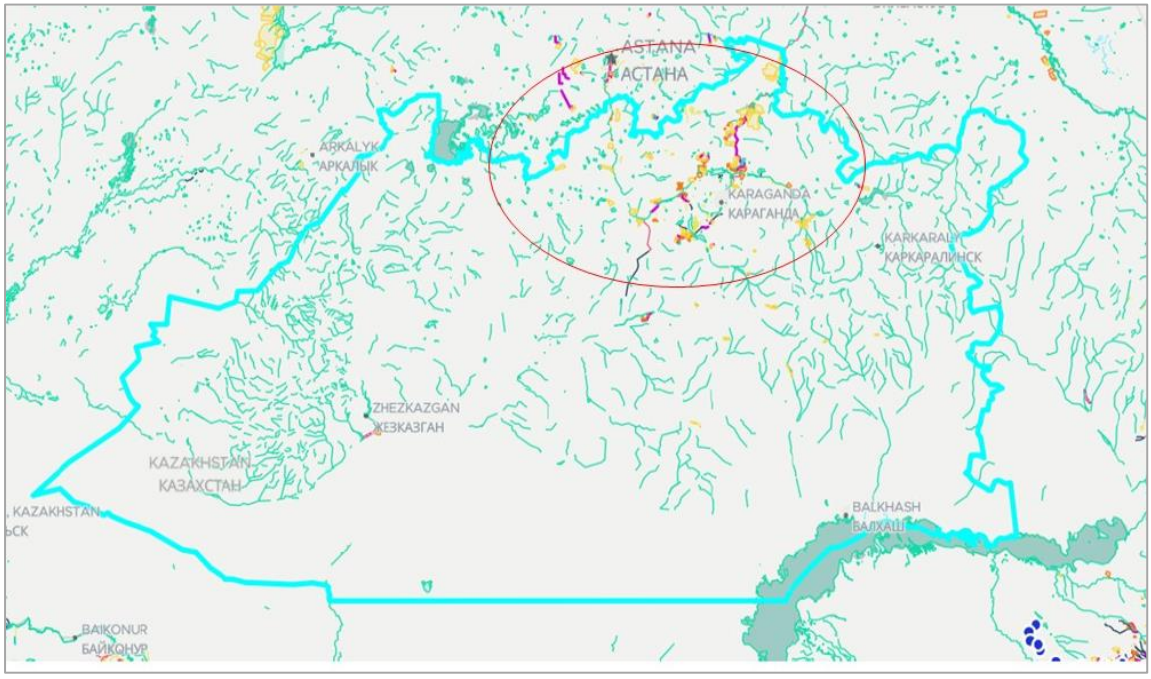

Figure 1: Location of irrigation systems in the Karaghandy province (the yellow areas within the red circle, province boundary shown in blue); Source: IEE (2019) and IWMI estimates.

IV. WATER PRODUCTIVITY ASSESSMENT

A. Background: Site Description

14. Karaghandy is the largest province of Kazakhstan covering over 15% of the country’s total land area. The province had diverse topography with elevation varying from 500m to 2000m above mean sea level, with the smaller mountain ranges of Kazakhstan located in the province. Karaghandy is dominated by plains, hills, low mountains and depressions filled with salt lakes. The soil cover in the region is very diverse, as is the climate, topography and vegetation. Steppe and desert are predominant soil types. Loamy

chernozem soils are found in the northern part of the province where majority of the cultivated areas are located, and to the south the soil type becomes brown desert-steppe soil as climate becomes drier.

15. The climate of Karaghandy is very variable due to the vastness of the territory; large annual and daily temperature ranges are experienced and the climate is highly variable on a year to year basis. Summer months are very hot, with the air temperature often rising up to 48°C; in contrast in winter it is very cold and frosty. The north Karaghandy on an average has more than 200 sunny days (with an average daily air temperature above 0°C) and south Karaghandy has more than 240 sunny days.

16. The average annual precipitation in the Karaghandy province ranges from around 130 mm to 300 mm; in the north east (the major agricultural region) precipitation during the April to October dry season averages around 250-300 mm and, in the south (the desert zones) around 60-80 mm during the same season. Evapotranspiration exceeds precipitation by 3 to 4 times during the summer months (IEE, 2019).

17. The Karaghandy province includes the Nura-Sarysu, Balkhash-Alakol, Ishim, Irtysh and Tobol-Torgai river basins. The density of the river network decreases from north to south depending on the terrain. Eleven rivers have a length of more than 100 km including; Nura (978 km), Torgai (827 km), Sarysu (800 km), Shiderty (502 km), Uly-Zhylanshyk (422 km), Kulanotpes (364 km), Kalmakgyrgan (325 km), Tuyndyk (303 km), Tokyrain (298 km), Jarly (193 km), and Taldy (129 km). In addition, there are over 500 water bodies including 107 rivers, 83 lakes, and 409 artificial reservoirs, and dams with hydraulic structures in the province (IEE, 2019).

18. The snow-melt from high altitude glaciers feed the major river flow in summers, which is vital for irrigation. Irrigated agriculture is one of the largest contributors to the country's GDP. Agricultural output in Kazakhstan is hugely dependent on water availability from rainfall and snow melt in the rivers. Over the past years, agricultural productivity has been affected by droughts. In addition, desertification in some of the river basins has led to food scarcity in the past, and the irrigated area has been reduced from 2.1 million ha in the early 1990's to 1.5 million ha presently (Karatayev et.al., 2017).

19. Due to unavailability of irrigation system boundaries, we used Google Earth Pro to visually identify and select the larger contiguous irrigated areas in the five districts of Karaghandy province which were identified in the IEE Report (2019). Figure 2 represent digitization results of the irrigated areas.

20. Figure 3 presents the major crop types in the cultivated areas of the five districts of Karaghandy province. The data set is extracted from the NASA and USGSs Global Food Security-support Analysis Data (GFSAD) 1km spatial resolution. GFSAD data provides crop extent, irrigated vs rainfed with spatial distribution of the major crop types in both extents. As more than 70% of Karaghandy province cultivated areas harvest grain and legumes, therefore, after delineating irrigated areas manually we used GFSAD dataset to get a more general information of crop type in the selected district's irrigated areas. Figure 3 shows that wheat and barley are the most common crop types in the selected districts,

with wheat the most dominant crop type in the irrigated areas delineated (see Figure 2 and Figure 3).

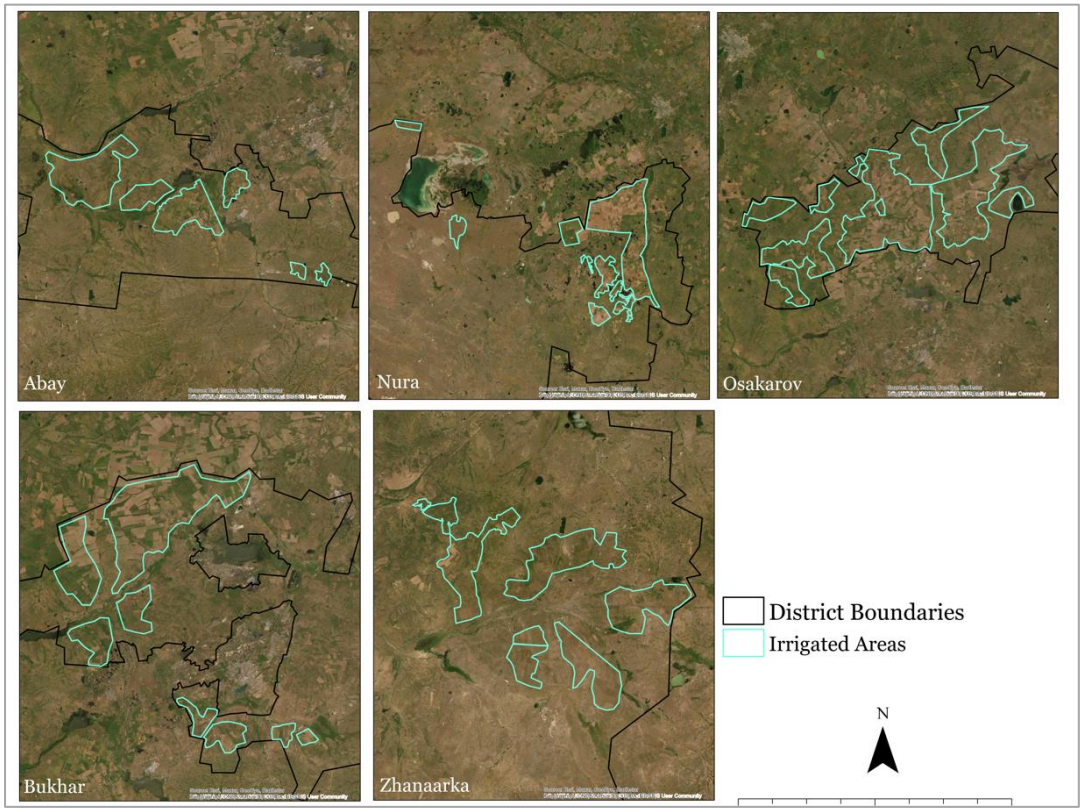

Figure 2: Irrigated areas delineated by visual interpretation from Google Earth, district boundaries shown with a black line.

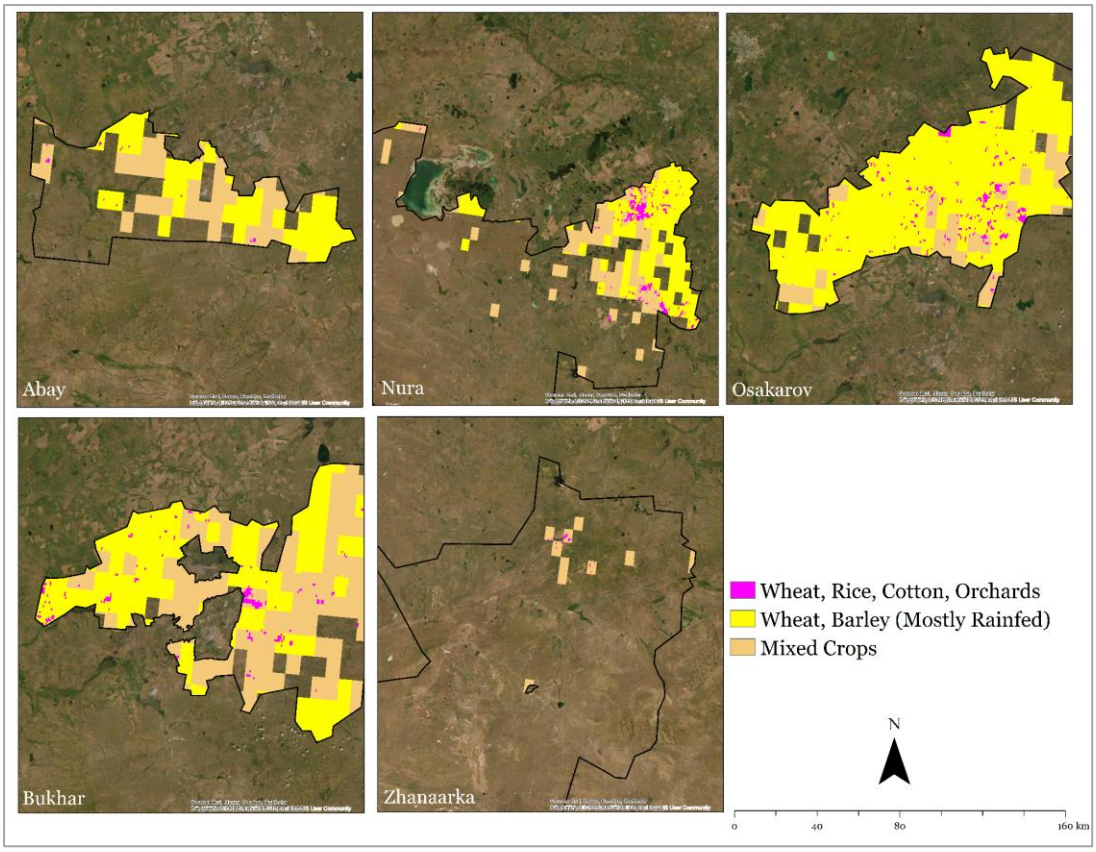

Figure 3: Crop classification for selected districts (Source: GFSAD 2020), district boundaries shown with a black line.

Table 1: Cropping systems in the Karaghandy region (Source: GFSAD 2020 and IWMI estimates)

Cropping system	Abay	Nura	Osakarov	Bukhar	Zhanaarka
Wheat, rice, cotton, orchards	N/A	41,600 ha (9%)	2,000 ha (<1%)	2,900 ha (<2%)	400 ha (<4%)
Wheat and Barley	32,800 ha (58%)	241,500 ha (53%)	568,800 ha (95%)	129,300 ha (76%)	N/A
Mixed crops including wheat	23,500 ha (42%)	172,900 ha (38%)	28,200 ha (<5%)	37,200 ha (22%)	10,400 (96%)

21. The irrigated areas in Kazakhstan have a wide growing season which starts from May and ends in October; the length varies from area to area with maximum green-up occurring late in the season (August-September) which is typically when irrigation water availability becomes critical (CACILM, 2009).

B. Summary of the approach

1. Methodology

22. SEBAL is a single-source model that uses visible, near-infrared and thermal infrared data collected mainly by sensors on board earth observation satellites

(Bastiaanssen, 2000). SEBAL has the advantage over conventional methods of estimating ET from crop coefficient curves or vegetation indices in that crop development stages do not need to be known, nor do specific crop types.

23. pySEBAL is a python based implementation of the SEBAL algorithm and auxiliary models (see IHE Delft and IWMI, 2020 and next section for details) which was used to translate raw satellite measurements into maps of actual evapotranspiration (ET_a) and Above Ground Biomass Production (AGBP), among others, for the Karaghandy region in Kazakhstan. This approach is dependent on the availability of cloud free satellite images (from the Landsat sensor) during the main growing season in selected areas.

24. pySEBAL is a python library to implement SEBAL using inputs from spatial data including spectral reflectances, climatic parameters, and altitude as inputs to estimate the surface energy balance components (Bastiaanssen et al., 1998a, 1998b). The outputs include parameters related to vegetation, energy balance, biomass, ET, and water productivity (Jaafar and Ahmad, 2020).

25. pySEBAL is provided as an open-source library with Apache version 2 license in a GitHub repository (https://github.com/wateraccounting/SEBAL). Currently, PySEBAL supports data from MODIS, Landsat, and Proba-V satellite sensors which facilitate the production of daily and seasonal ET_a maps. PySEBAL was deployed to compute ET_a and AGBP maps. The theory behind PySEBAL and the computation of ET_a and AGBP, as well as a full specification of the data requirements are detailed in the project methodology document manual (IHE Delft and IWMI, 2020); only data which are specific to the current analysis are provided here.

2. Data inputs

26. Spectral radiances in the visible, infra-red and thermal range of the electromagnetic spectrum are the main input to the SEBAL model. Data from the Landsat satellites are typically used for this purpose; the high spatial resolution (30m) of the data provides sufficient detail to characterize the spatial patterns of biomass production and water deficits across the command area, and the revisit time of 16 days can, under cloud free conditions, provide sufficient coverage of an irrigation season.

27. The main irrigated areas in Abay, Bukhar, Nura, Oskarov and Zhanaarka districts of the Karaghandy province are covered by six Landsat Tiles (row 25 paths 154, 155 and 156; and row 26 paths 154, 155 and 156)[1]. The district boundaries and Landsat image footprints covering the identifiable irrigation schemes is shown in Figure 4. An initial analysis was conducted on the images in the above mentioned paths and rows during three years (2017, 2018 and 2019). That analysis relied on percentage cover and distribution of clouds across the selected districts during each irrigation season. In conclusion, 2019 was selected for the current analysis. A total of 41 Landsat 8 images were downloaded and processed for 2019 growing season May to October (see Annex A for image details and Table 2 for cloud cover

[1] Note that the location of irrigation schemes has been identified visually from the IEE (2019) report and Google Earth due to the lack of digital data for subproject locations; there is a possibility that very small schemes have not been identified and are not included in the 6 Landsat Tiles.

summary of the images selected for analysis). Images with a threshold of less than 75% cloud cover on land were downloaded and further interpreted to ensure the images with low cloud cover had usable data over the selected districts.

Table 2: Seasonal average cloud cover for selected Landsat 8 OLI images used for this analysis.

R25P154	R025P155	R25P156	R26P154	R26P155	R26P156
36%	47%	38%	37%	35%	36%

28. A time-series of meteorological parameters at the time of satellite data acquisition (instantaneous) and the 24-hour average representing the day of acquisition are required to implement the pySEBAL model; these are needed to calculate the soil water balance and Penman Monteith Standard Reference Evapotranspiration (see IHE Delft and IWMI (2020) for full details).

29. Instantaneous (hourly) and daily average data from the NASA Global Land Data Assimilation System (GLDAS 2020) were acquired for the command areas and used as input to the pySEBAL model. GLDAS is an assimilated global data product from satellite and ground-based observations, with data available at 0.25-degree spatial resolution and at 3 hourly intervals. The parameters used are listed in Table 3.

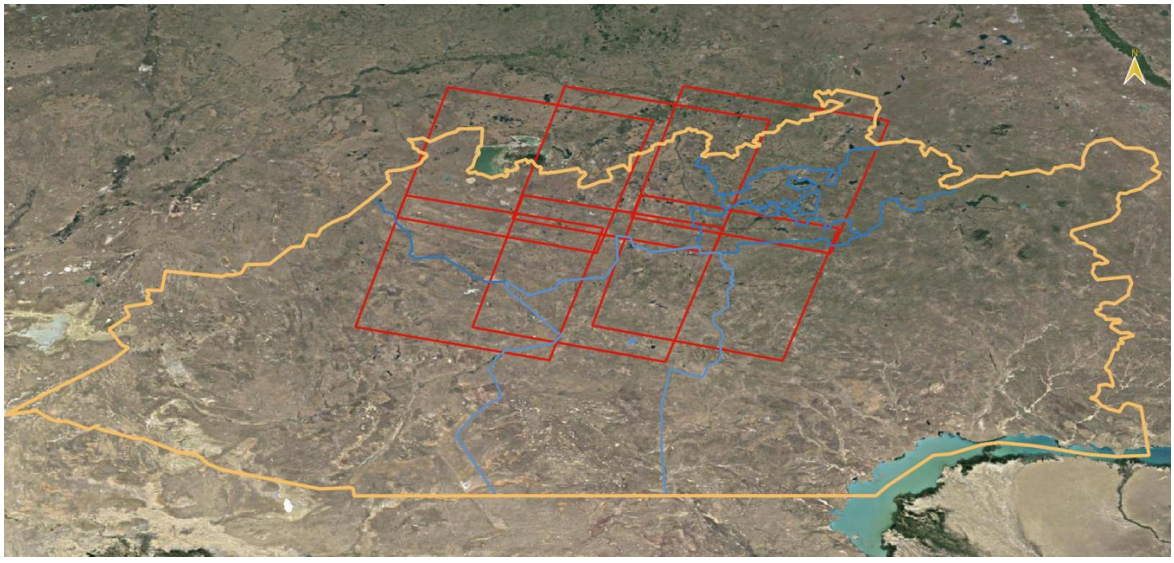

Figure 4: Location of the Karaghandy province boundary (yellow), district boundaries (red), and Landsat tile footprints (blue); Source: Google Earth and IWMI estimates.

30. The preprocessing of meteorological data includes following steps: i) extract the variable and clip to study area, iii) converting the units of air temperature from Kelvin to °C, pressure from Pascal (Pa) to Millibar (mb) and specific humidity in kg/kg to relative humidity in % and iv) extracting instantaneous and daily average meteorological variables from three-hourly data. The instantaneous data corresponding to the Landsat acquisition time (10:30 A.M local time) is estimated by averaging the 6H and 9H outputs from GLDAS, while

all the 8 images in a day are averaged to estimate 24 hours' data representing the day of Landsat acquisition.

Table 3: Meteorological data inputs to the PySEBAL model

Parameter	Symbols	Unit
Downward shortwave radiation	SWdown	W/m^2
Wind speed	Ws	m/s
Air temperature	Tair	°C
Pressure	P	Mb
Relative humidity	Rh	%

31. A Land use/land cover (LULC) map or a map depicting the location of irrigated areas, or boundaries of the irrigation system, is needed to ensure that the analysis is limited to the relevant areas. The data presented in Figure 3 are used for this purpose.

32. Following the collection and preparation of the various input datasets, the pySEBAL model was implemented following the steps shown in Figure 5. The acquired Landsat 8 data was pre-processed to create cloud masked Top Of Atmosphere (TOA) reflectance bands. The pre-processing includes conversion from Digital Number (DN) to TOA reflectance, cloud removal using the Quality Assessment (QA) band provided along with the data. All the satellite data pre-processing was done inside pySEBAL (Steps 1, 2 in Figure 5).

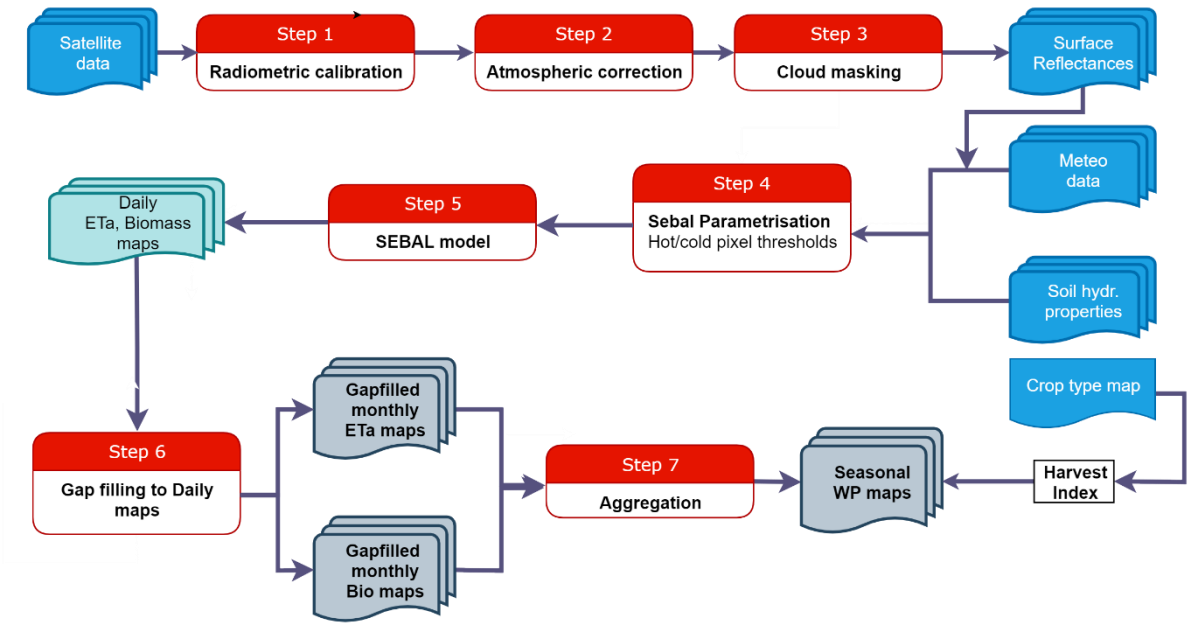

Figure 5: The pySEBAL methodological framework for WP assessment.

3. Cloud masking and gap filling

33. The images used in analysis had cloud cover of varying amounts (see Table 2 and Figure 6); acquiring a total cloud free image from a low temporal frequency satellite such as Landsat is challenging (Nugent, 2018). It was thus necessary to include images with partial cloud cover in the analysis, where cloud free portions within those images are present in particular over the irrigated areas. Although, the climate of the Karaghandy region is very dry and the average cloud cover during the growing season was less than 40% in most areas (see Figure 6), cirrus clouds (high altitude, thin layer of non- precipitation clouds) were present which affect the image quality. Therefore, following cloud masking of the input data, the outputs from pySEBAL required spatial gap filling.

34. Given the Landsat revisit time of 16-days, combined with the presence of cloud cover, it is frequently the situation that only one image is available per month. To calculate the seasonal estimates of ET_a and AGBP temporal gap filling is thus also required.

35. Spatial gap filling was performed for cloud masked areas in the pySEBAL output through an interpolation process; following this, Locally Weighted Regression (LWR) based temporal interpolation method was employed to fill the gaps in the monthly outputs (for ET_a and AGBP) using GRASS GIS 7.8 software (Metz et al., 2017). This method fits a time series model for each pixel in monthly raster images and interpolates the missing values using neighbouring observations. Some gaps continue to persist in monthly outputs after the application of LWR temporal interpolation method due to insufficient valid observations in the time series. A bicubic spline based spatial interpolation which uses the neighbouring 16 pixels around the null pixel was applied to the individual LWR interpolated maps to fill the remaining gaps (Neteler, 2010). Gap filled monthly rasters of ET_a and AGBP were aggregated over the growing season (May to October) to derive seasonal outputs.

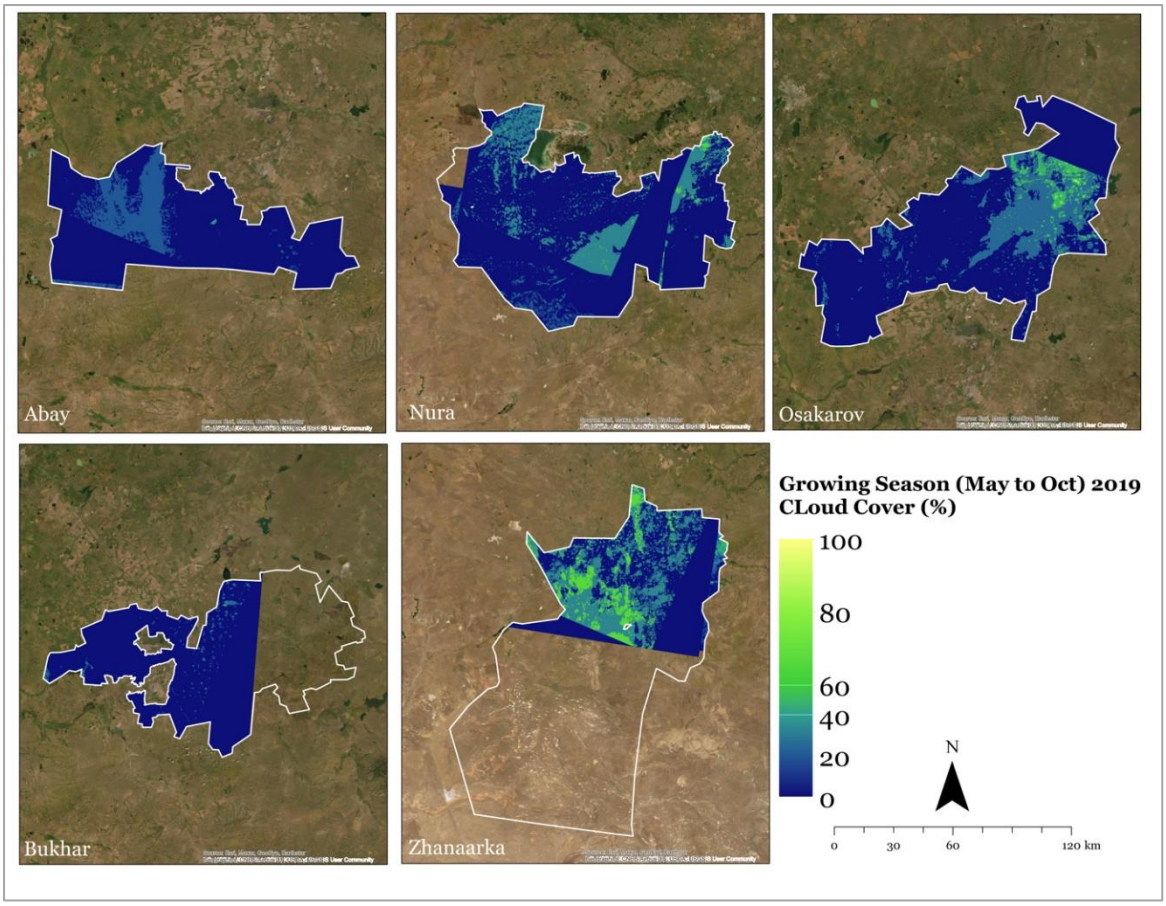

Figure 6: Cloud cover percentages during the growing season of 2019 (May to October) for the irrigated areas of selected districts.

4. Water Deficits and Gross Biomass Water Productivity

36. Following the gap filling of the pySEBAL outputs (the ET_a and AGBP), two further parameters are calculated; these are the relative water deficit (RWD) and the Gross Biomass Water Productivity (GBWP).

37. RWD is a direct expression for any water shortage the crop is experiencing on a pixel by pixel basis, and it can help to assess (without any further information on canal flows) whether the crop has sufficient moisture in the root zone. This information is useful in understanding and interpreting irrigation performance across a command area. The RWD index can be used to identify areas that suffer the most from lack of irrigation water availability and access, as it broadly shows where irrigation water has been insufficient to meet the crop water requirement (Steduto et al., 2012); assessment of this index can provide insights into deficit conditions across the command area for a particular crop, over the irrigation season. The RWD often correlates with other biophysical parameters such as biomass and ET_a. For example, regions with high RWD translate to low crop biomass production, which in turn gives an indication of the areas where there are yield losses due to limited water supply.

38. The RWD was calculated according to Equation 1, where ET_a/ETmax is the ratio of the actual ET in mm (based on the satellite images and derived through the pySEBAL model) to the ETmax in mm. ETmax is the 99th percentile of the actual ET in the irrigated areas (see IHE Delft and IWMI 2020 for full details).

$$RWD = (1 - \left(\frac{ETa}{ETmax}\right))$$

Equation 1

39. The second parameter calculated from the pySEBAL outputs is the GBWP. This represents the total amount of biomass produced in relation to the actual crop water consumed during the growing season. It is defined following the Equation below, where AGBP is in kg/ha and ET_a is in m^3/ha.

$$GBWP = \left(\frac{AGBP}{ET_a}\right))$$

Equation 2

40. It should be noted that a major assumption is that wheat is the dominant crop in all of the irrigated systems analyzed (see Figure 3 and Table 1).

C. Presentation of Results

41. The outputs of the analysis (the ET_a, RWD, AGBP and GBWP) are intended to be used to inform and assist in the identification and prioritization of opportunities to improve the productive use of water through improved water supply within the major irrigated wheat growing areas of the Karaghandy region. The results presented are for the 2019 growing season (May to October) and for the irrigated areas delineated (see Figure 2) for selected districts, both as district level summaries and subsequently the spatial data for each parameter.

1. District summaries

42. Table 4 presents the seasonal mean values for the water consumed (ET_a), the RWD, AGBP and GBWP in the irrigated areas of the five districts, Abay, Bukhar, Nura, Osakarov and Zhanaarka.

43. The mean seasonal ET_a is relatively low compared the remote sensing based analysis of other wheat areas in Asia. For example, Cai et al (2018) estimated mean seasonal ET_a for wheat in Madyha Pradesh in India[2] to be 318 mm. This is expected due to limited water availability and the arid climate during this season. The high coefficient of variation (Table 4) means high variability across the area which is expected given the arid climate and low and low dry season precipitation, and the dilapidation of the irrigation systems.

44. Irrigated areas in Osakarov exhibit the highest mean ET_a (297 mm), while Nura demonstrates the lowest (211 mm). The AGBP demonstrates the same pattern, with highest mean values estimated for Osakarov (8,071 kg/ha) and low values estimated for Nura (7,010 kg/ha). Zhanaarka demonstrates similar mean ET_a (218 mm) to the Nura district, but much lower mean AGBP (4,468 kg/ha which is the lowest among the five districts). This may be due to various reasons including the smaller, more fragmented agricultural areas within the district, the prevalence of a different cropping system (grains and legumes, see Figure 3), or as a result of faltering irrigation systems or management of irrigation water.

Table 4: Spatial mean of the seasonal values of ET_a, RWD, AGBP and GBWP in the irrigated areas of Abay, Bukhar, Nura, Osakarov and Zhanaarka. Coefficient of Variation is displayed in brackets.

	Mean ET_a (mm)	**Mean AGBP (kg/ha)**
Abay	278 (55%)	8,037 (46%)
Bukhar	239 (47%)	7,739 (38%)
Nura	211 (80%)	7,010 (57%)

[2] While the ET_a figures should not be compared across regions as the analysis is location specific, they provide a ballpark figure for relative comparisons

Osakarov	297 (42%)	8,071 (42%)
Zhanaarka	218 (68%)	4,468 (71%)

The frequency distribution of the estimated ET_a during the 2019 irrigation season is presented in Figure 7 for the irrigated areas in each district. While all districts have a wide range of values (from 0 to over 700 mm), the frequency of pixels with higher values than the mean is highest in Osakarov and lowest in Nura and Zhanaarka. Overall, the distributions are unimodal, and right skewed except Osakarov. Thus all districts except for Osakarov have large areas (more pixels) where seasonal water consumption is lower than the district mean value.

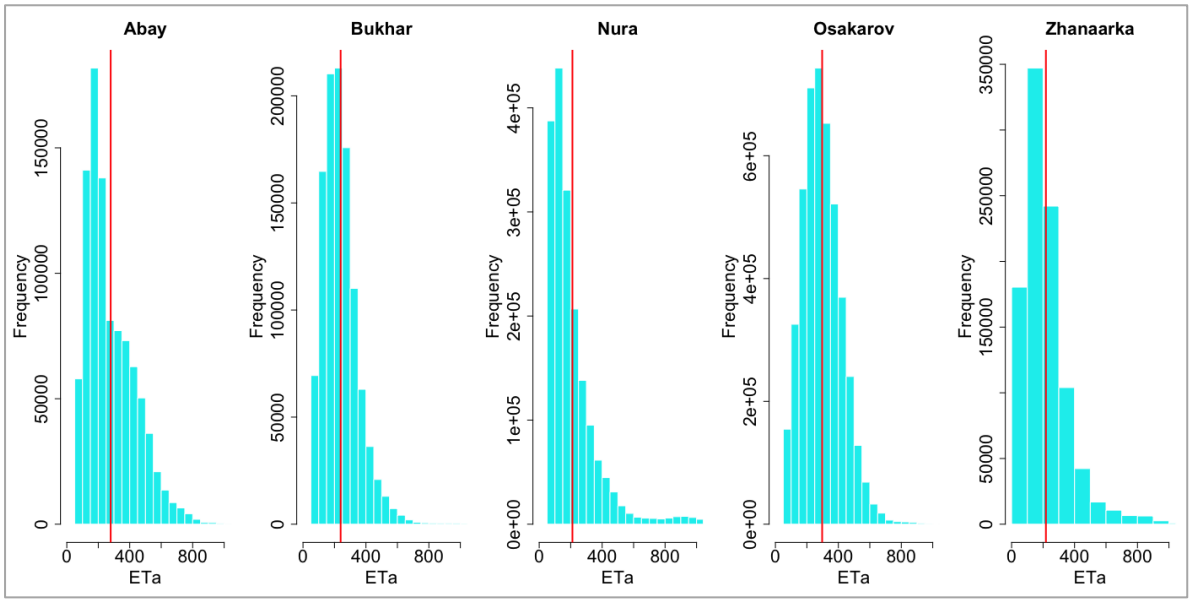

Figure 7: Frequency distribution of seasonal ET_a for the irrigated areas of the selected districts in the Karaghandy province. The red line indicates the mean value.

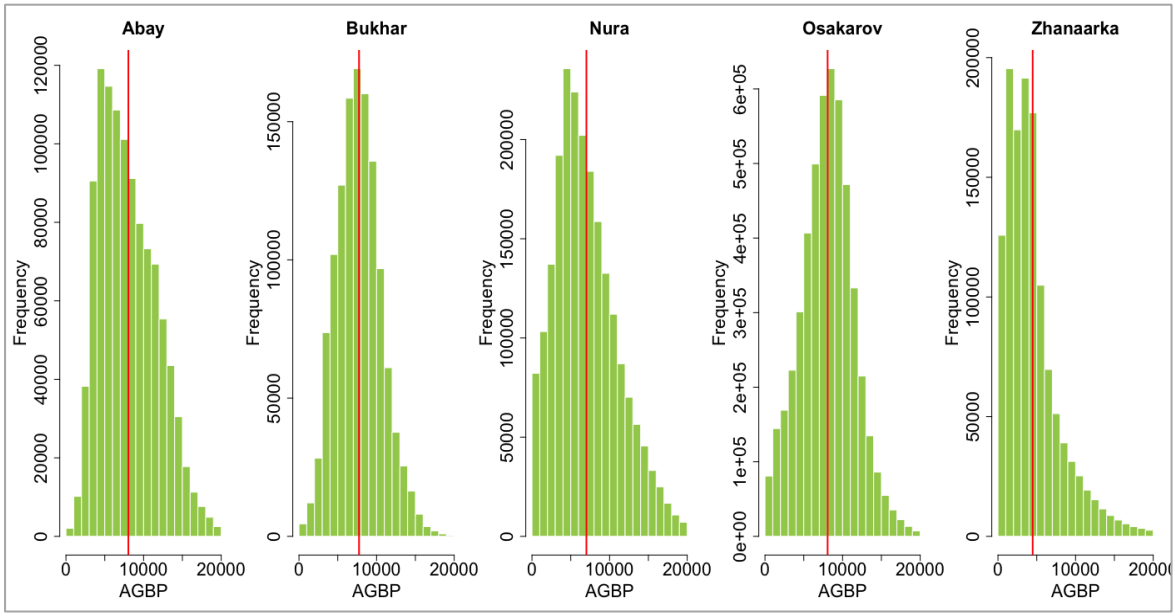

Figure 8: Frequency distribution of seasonal AGBP for the irrigated areas of the selected districts in the Karaghandy province. The red line indicates the mean value.

45. The frequency distribution of the estimated AGBP values during the 2019 irrigation season is presented in Figure 8 for the irrigated areas in each district. All districts have a wide range of values (from 0 to over 18,000 kg/ha); the frequency distributions are unimodal and are normally distributed, except for Zhanaarka and Abay, which have a larger number of pixels with values lower than the mean. Interpreting the reasons for this distribution requires an assessment of the spatial data; this is done in the following sections.

2. Maps of water productivity parameters

46. The results presented in the previous section provided the mean values estimated for the major irrigation areas summarized at the district level. The spatial data (the maps) for each parameter provide more detail, as they enable us to see patterns within, as well as between the irrigation areas. The maps are presented and discussed in the following paragraphs.

3. The Abay District

47. Figure 9 presents the maps of spatial distribution of ET_a, RWD, AGBP and GBWP in the Abay district of the Karaghandy province. Wheat is the most dominant crop during the irrigated season, but barley and mixed crops (vegetables) may also cultivated (see Figure 2 and Figure 3). The areas in the largest block of irrigated lands in the north west of Abay had lower ET_a among other irrigated areas except for some irrigated fields closer to a water channel in the southern portion of the block. Given the low levels of water consumption and low AGBP over the season, it is unlikely that an irrigated crop was grown in much of this block. In contrast the larger block in the center demonstrates higher values of ET_a and AGBP, mostly in the eastern side of the block; these values suggest higher performance of the irrigation systems in this location.

48. Similarly, in other blocks, the areas with higher ET_a values are those located closer to water channels. These are also the areas with higher AGBP and consequently lower RWD values, and higher GBWP values. Overall the central blocks had higher ET_a and AGBP, and lower RWD while the north west block had low ET_a, low AGBP and higher RWD, except for isolated areas in the southern part of the block. Although, a trend of higher ET_a, lower RWD and higher AGBP is observed in areas closer to the water channels, surprisingly the irrigated areas closer to an apparent water channel in northern side of the north west block had higher RWD and lower AGBP, which may indicate that it is dysfunctional and thus be due to issues with water delivery.

49. The larger of the two central blocks is the Koksun project, which is fed by the Zhartas reservoir (visible in the southwest corner of the block; this is one of the Subproject locations in Abay (IEE, 2019).

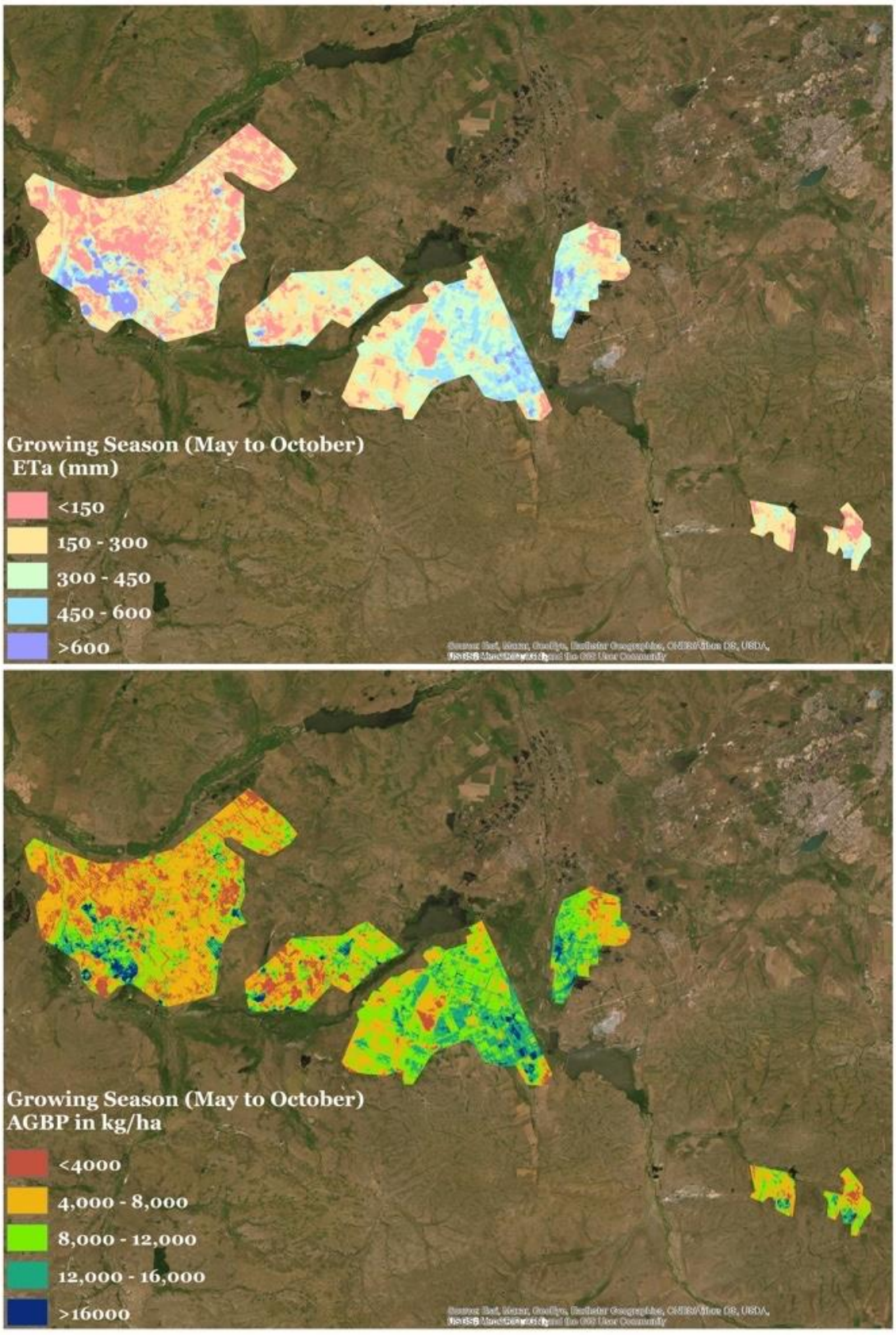

Figure 9: ET_a, and AGBP for the irrigated areas of the Abay district in the Karaghandy province during May to October 2019

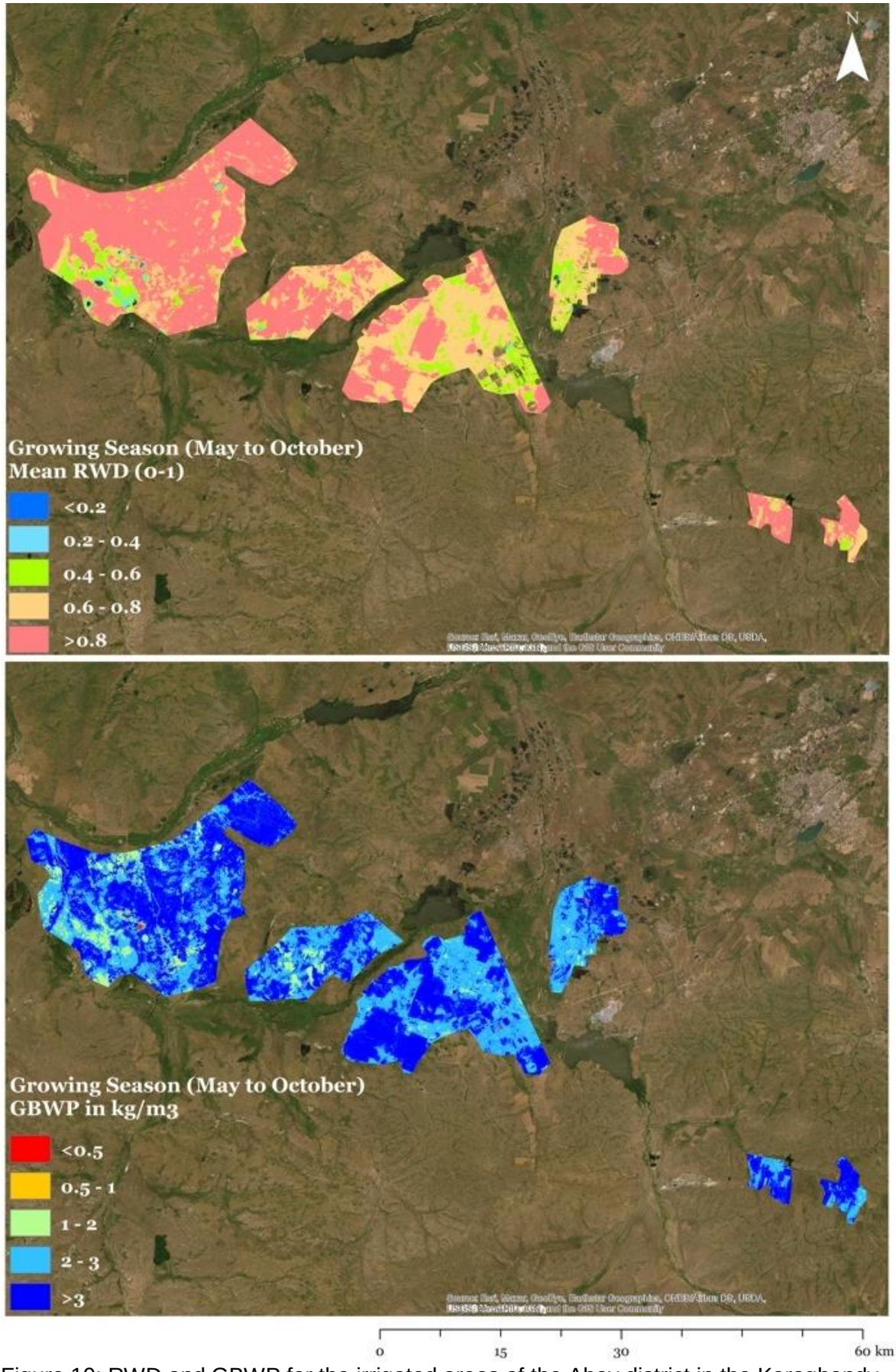

Figure 10: RWD and GBWP for the irrigated areas of the Abay district in the Karaghandy province during May to October 2019

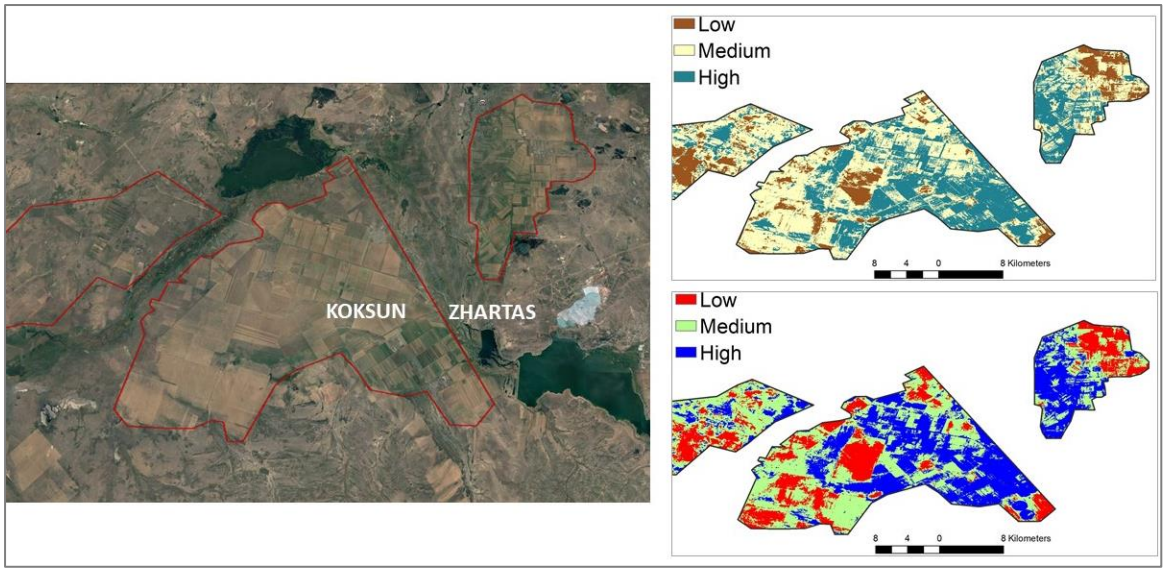

Figure 11: Zhartas reservoir and Koksun irrigation system; ET_a top right, AGBP bottom right. Source: Google Earth and IWMI estimates.

50. Figure 11 shows the ET_a and AGBP estimates for the Subproject site, classified into low, medium and high categories for each parameter. While both ET_a and AGBP vary spatially within the irrigation scheme, there is a clear pattern of higher values near the outlet of the reservoir and in the head section of the scheme. To the north of this a declining trend in ET_a and AGBP is evident; and the western portion of the scheme furthest away from the reservoir is under performing in comparison to the southeast. In addition, there is a section in the middle of the scheme (the brown area in the top right panel and the red area in the bottom right panel) which demonstrates much lower values than the surrounding areas. This suggests that there is likely to be an issue with water delivery to this parcel.

4. The Bukhar District

51. Wheat, barley and mixed crops (vegetables) are the dominant crop types in this district (see Table 1 and Figure 3). The seasonal ET_a across the majority of the irrigated areas in the district is in the range of 300 to 400 mm. Isolated and scattered areas of lower mean RWD, higher ET_a and higher AGBP are evident in the maps presented in Figure 12. The linear pattern of blue areas (higher ET_a) in seasonal ET_a map in Figure 12 suggests that the fields closer to distribution channels have higher levels of water consumption. Overall the northern irrigated areas had higher ET_a, AGBP, GBWP and lower RWD. These areas are predominantly wheat growing regions.

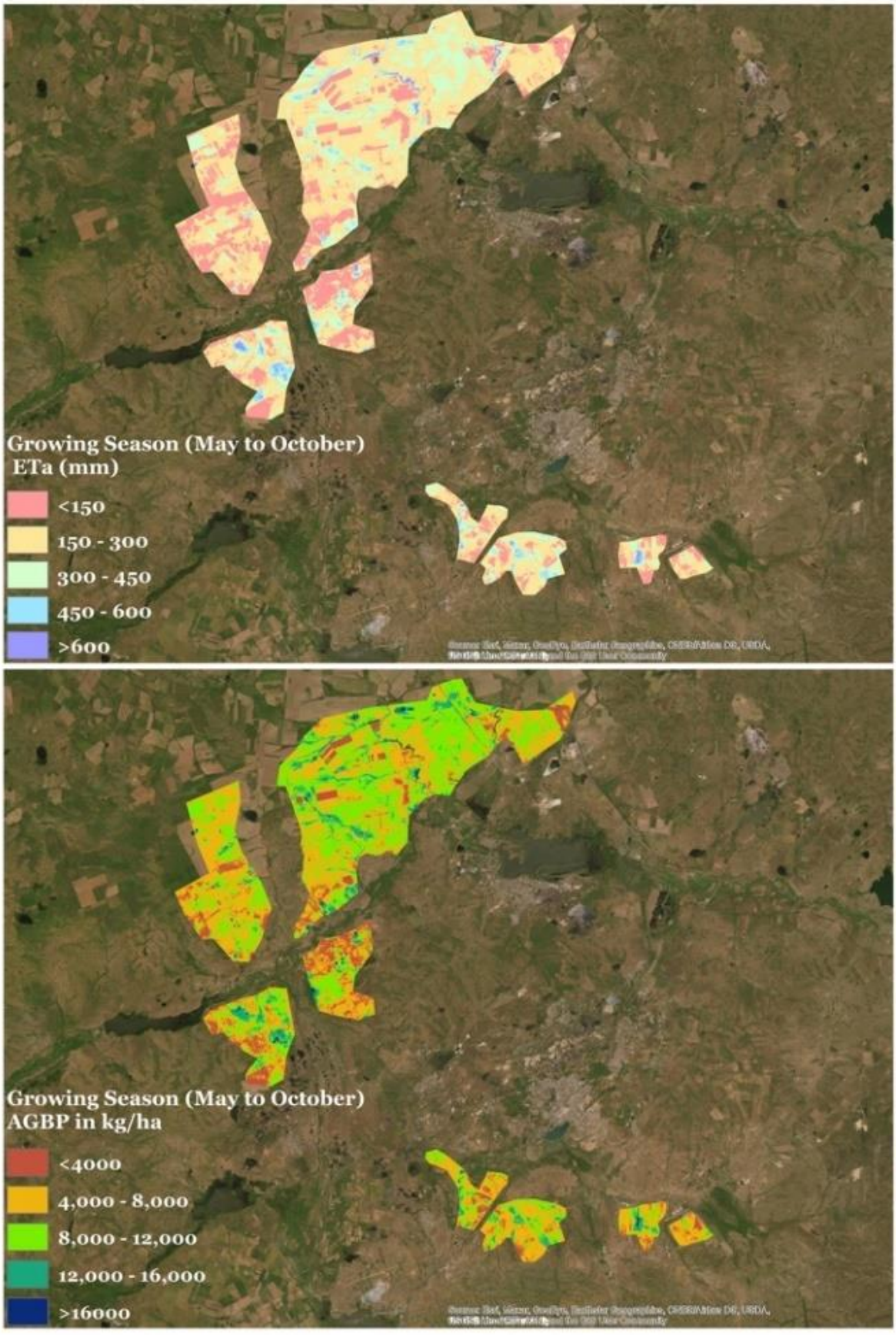

Figure 12: ET_a, and AGBP for the irrigated areas of the Bukhar district in the Karaghandy province during May to October 2019

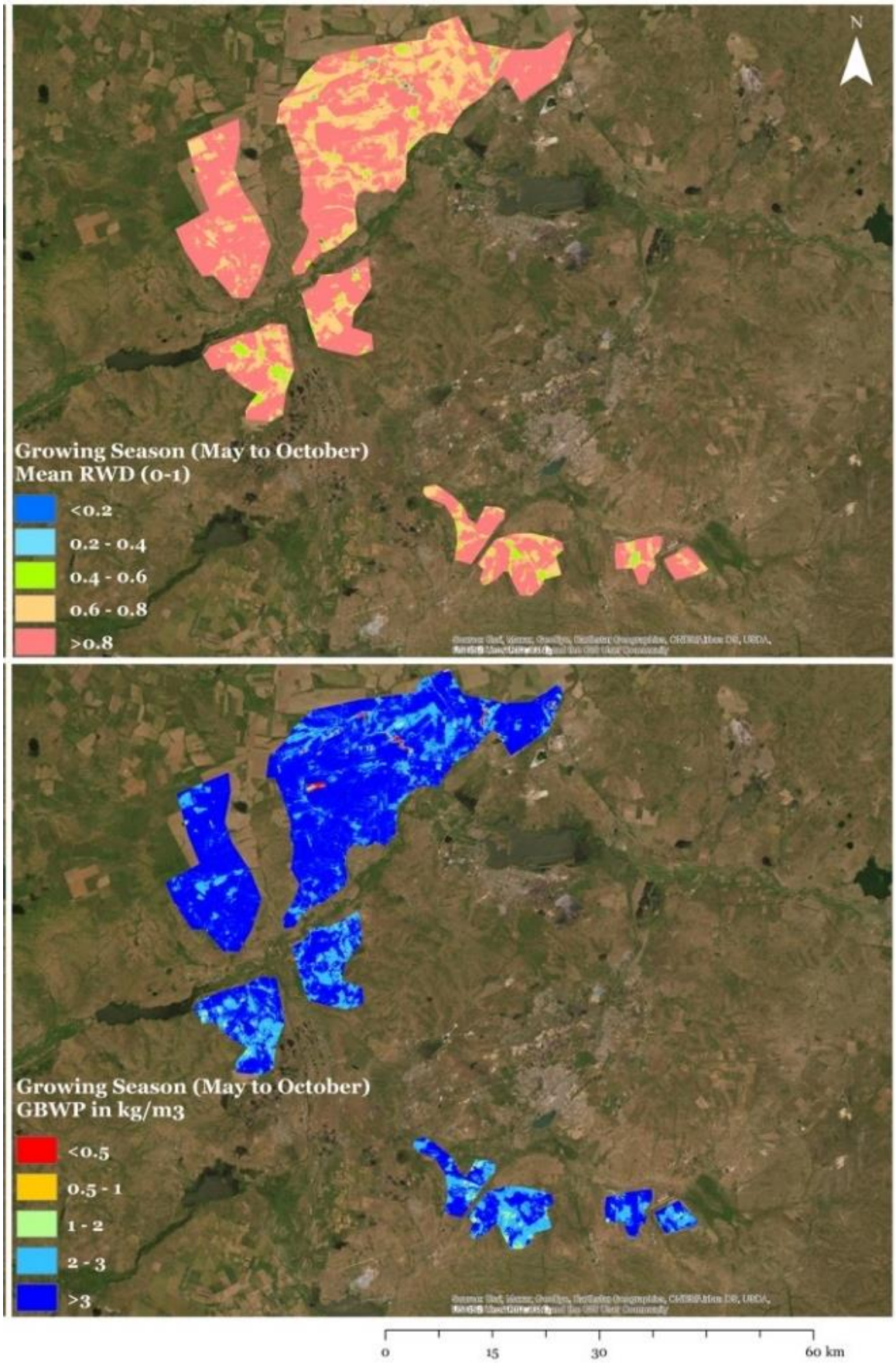

Figure 13: RWD and AGBP for the irrigated areas of the Bukhar district in the Karaghandy province during May to October 2019

5. The Nura District

52. Wheat, barley and mixed crops (vegetables) are cultivated in the irrigated areas of Nura (see Table 1 and Figure 3). Wheat is the dominant crop in these irrigated areas. The spatial data are presented in Figure 14; within this, it is apparent that there are some spots of higher ET_a (purple areas >600 mm) in the north of Nura; these are most likely from small water bodies surrounded by irrigation, as can be seen from the basemap in the figure. There is no dominant spatial pattern in the irrigated areas, which are typically showing low ET_a and high deficits, however the AGBP is higher in northern part of the larger irrigated block than in south of the block.

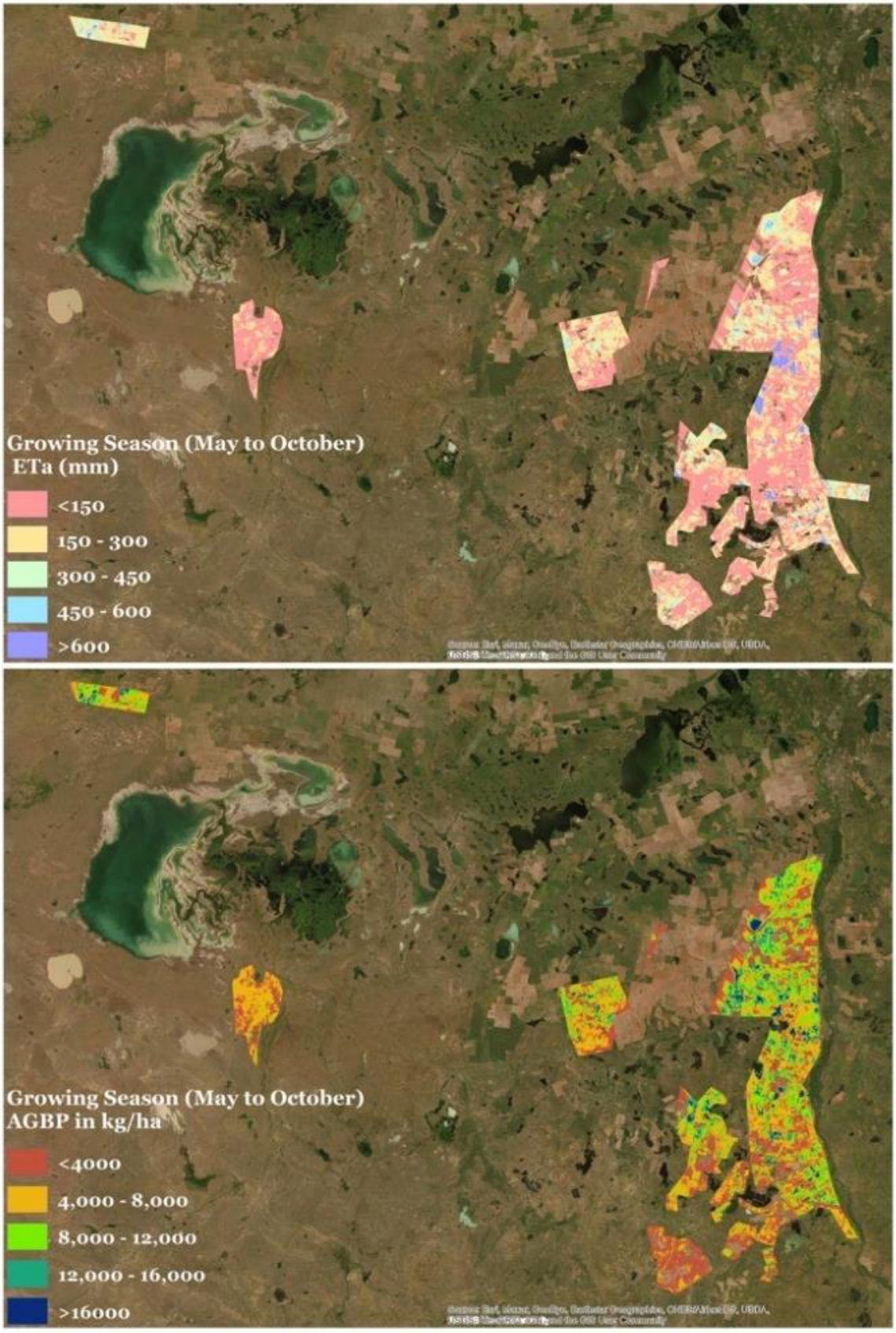

Figure 14: ET_a, and AGBP for the irrigated areas of the Nura district in the Karaghandy province during May to October 2019

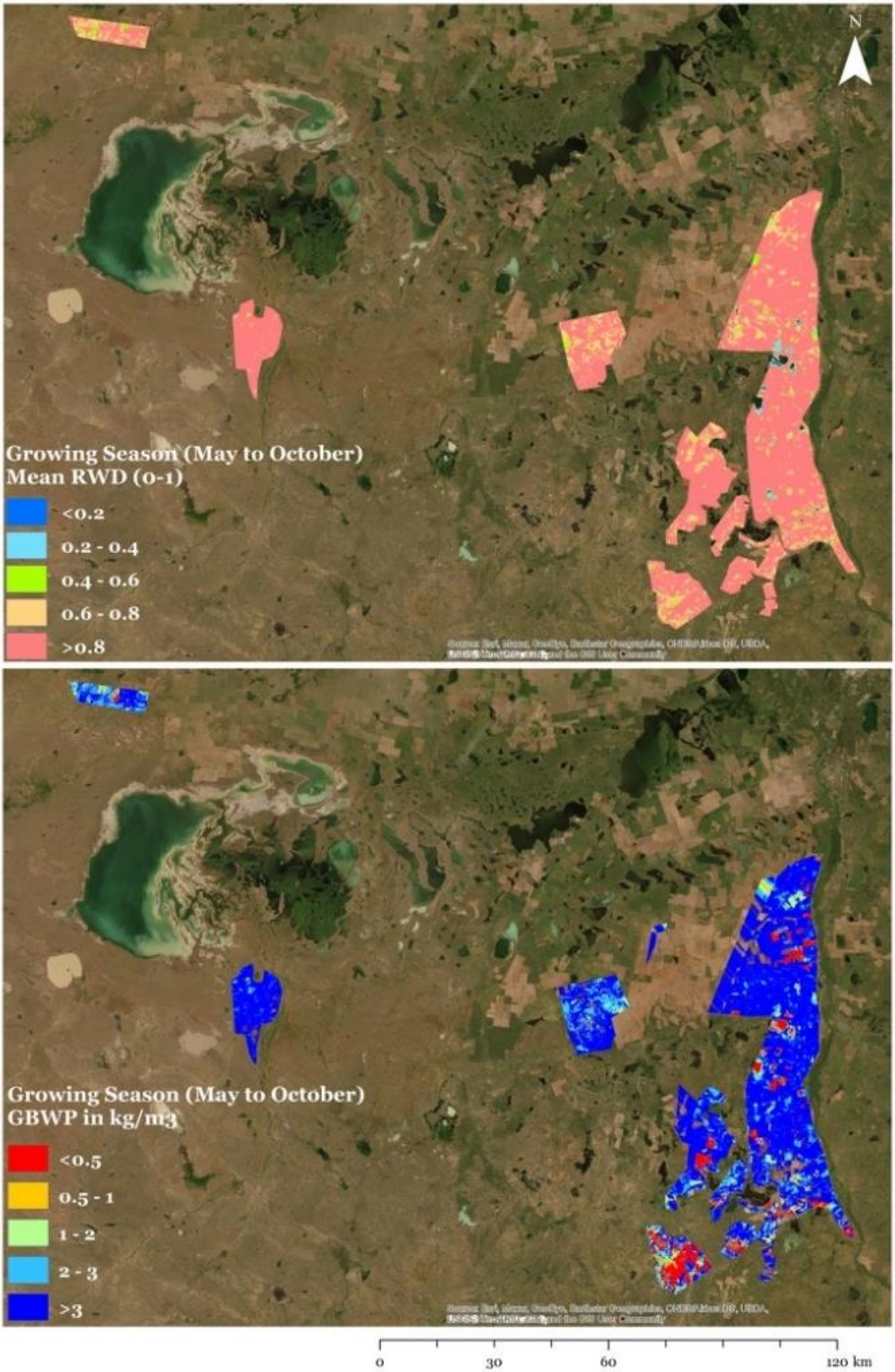

Figure 15: RWD and GWBP for the irrigated areas of the Nura district in the Karaghandy province during May to October 2019

6. The Osakarov District

53. Wheat and barley are the dominant crops types in the Osakarov district. Osakarov had the largest areas of irrigation compared to the other districts in the Karaghandy province. The spatial distribution of seasonal ET_a (Figure 16) shows that the irrigated areas in the center and north east of the district had higher ET_a (400-600 mm, the blue areas) than rest of the district. The areas on the far east side of the district had higher deficits and lowest AGBP values. Fallow fields are clearly visible as the red-brown areas in the AGBP map (Figure 16). Other than the northeastern block, these are typically isolated fields surrounded by higher performing areas.

54. The locations of low and high ET_a visible in Figure 16 are likely a results of variability in irrigation water supply. The IEE (2019) report lists several canals to be rehabilitated in this area; the possible locations of three are identifiable on Google Earth (Tuzdy, Samarkandsii, and Gagarin, Figure 18). Based on these it seems that the irrigation systems are fed by the Tuzdy reservoir in the south, with the central portions of the identified irrigation blocks fed by the main canal. Categorizing the ET_a and AGBP into low, medium and high categories (Figure 18) highlights the spatial variations, with areas of low water consumption and biomass production located in the east and west extremes, and more productive areas located in the central portions. This pattern is likely due to dysfunctional sections of canals in the locations with low ET_a and low AGBP values.

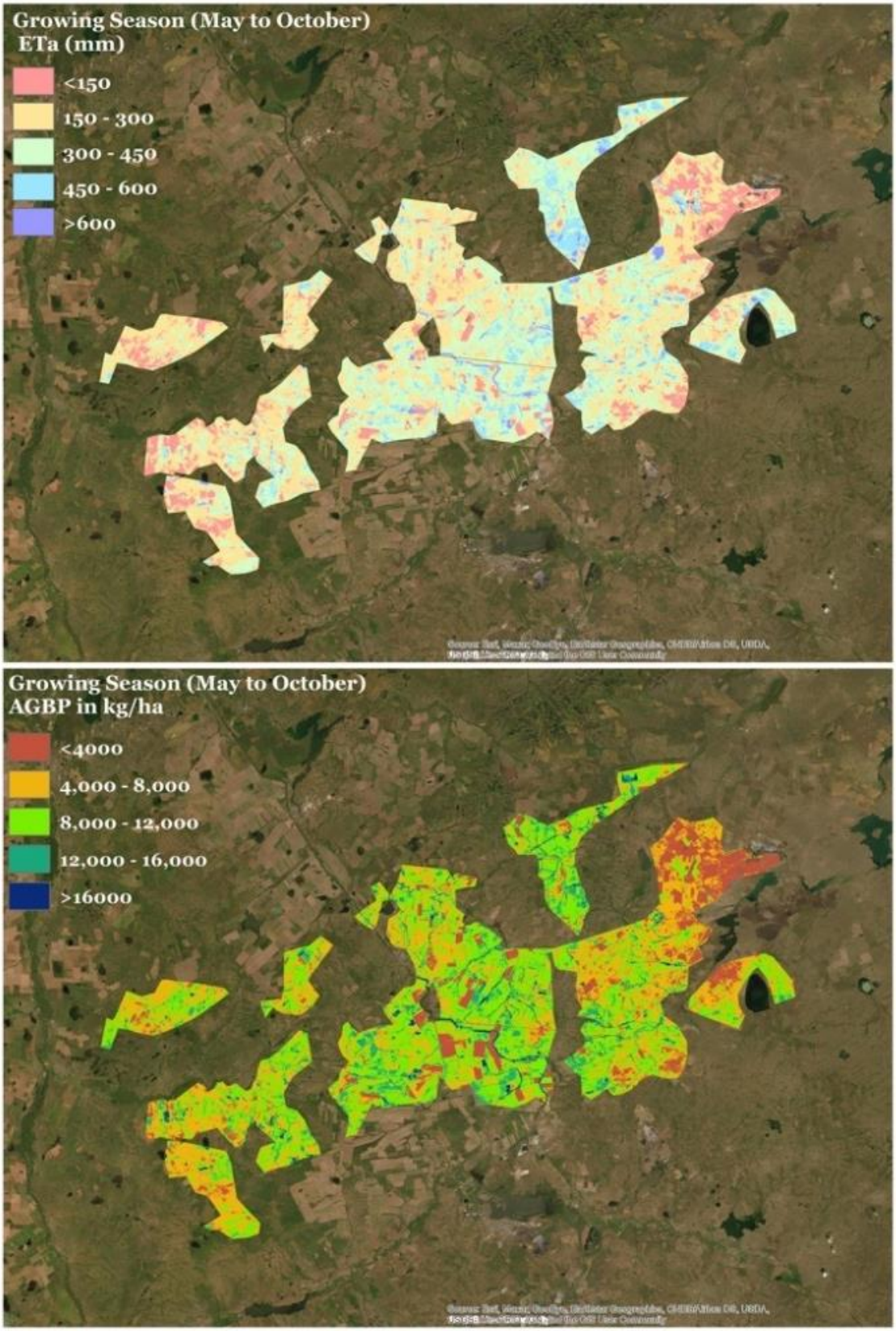

Figure 16: ET_a, and AGBP for the irrigated areas of the Osakarov district in the Karaghandy province during May to October 2019.

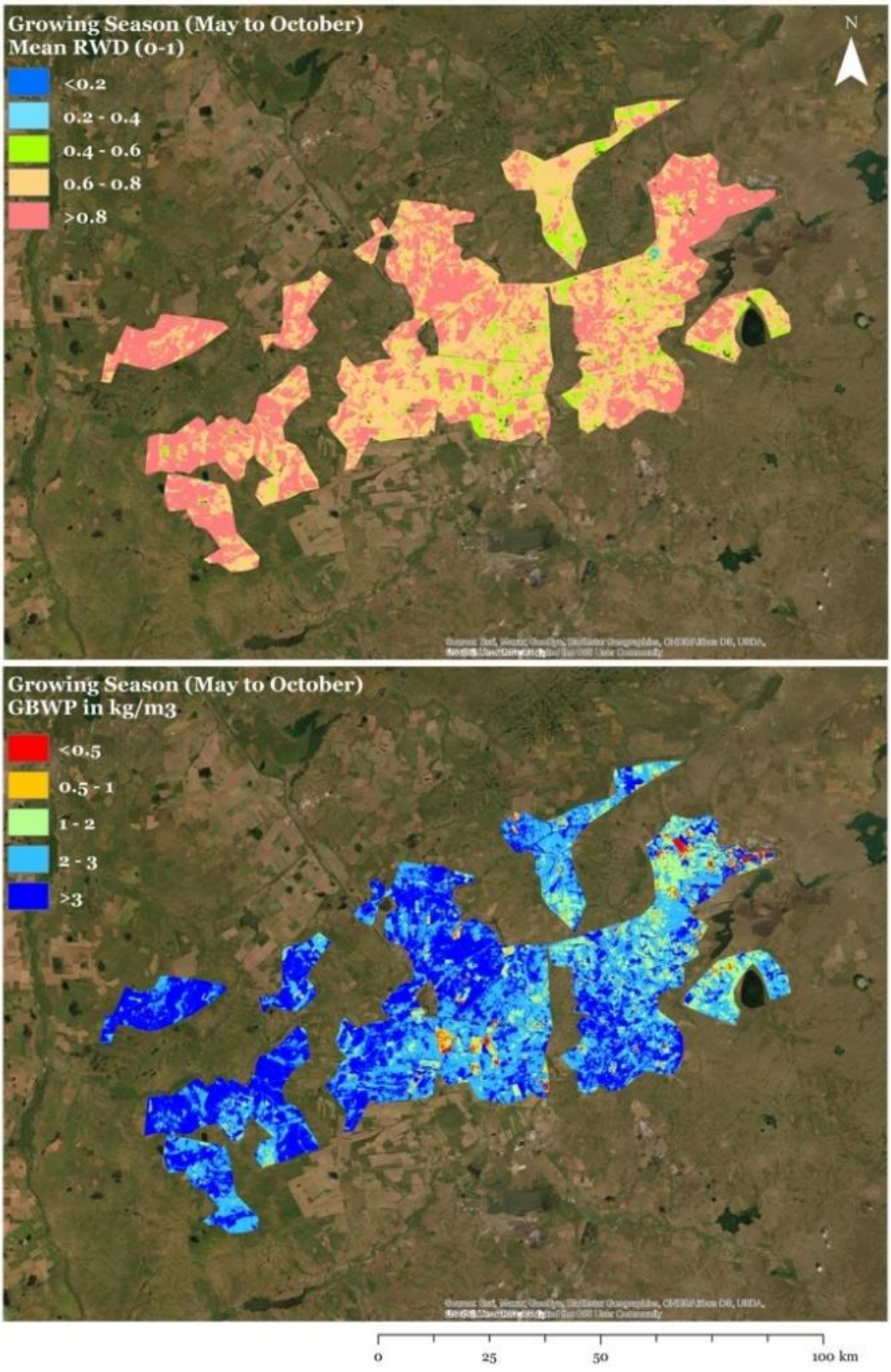

Figure 17: RWD and GWBP for the irrigated areas of the Osakarov district in the Karaghandy province during May to October 2019.

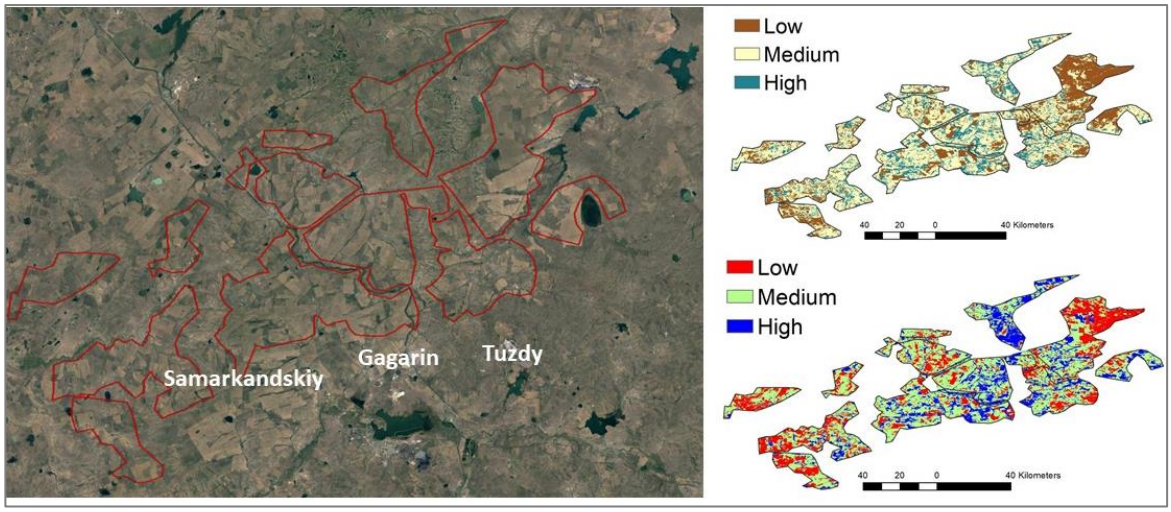

Figure 18: Possible Subproject locations (left image); seasonal ETa (top right), seasonal AGBP (bottom right). Source: Google Earth and IWMI estimates

7. The Zhanaarka District

55. Figure 19 presents maps of spatial distribution of ET_a, RWD, AGBP and GBWP in Zhanaarka district of the Karaghandy province. The available information from GFSAD crop classification dataset only listed mixed crops in the Zhanaarka district (see Figure 2 and Figure 3). Zhanaarka district is part of south Karaghandy province where there are sandy soils and desertification is more common. The spatial distribution of ET_a (Figure 19) reveals that in general the northern blocks have very low levels of water consumption, and are unlikely to be cultivated during the 2019 irrigation season. In contrast higher seasonal water consumption (higher ET_a values) are visible in the eastern block, and in a couple of isolated parcels of land in the western and central blocks. In particular, the southwestern portion of the eastern block demonstrates high ET_a (> 600 mm) and high AGBP (> 16,000 kg/ha) suggesting that this area received sufficient water during the dry season. Further assessment is required to determine whether these are higher performing irrigated areas, or whether they are areas of natural vegetation around water bodies which have been mis-classified as irrigated areas.

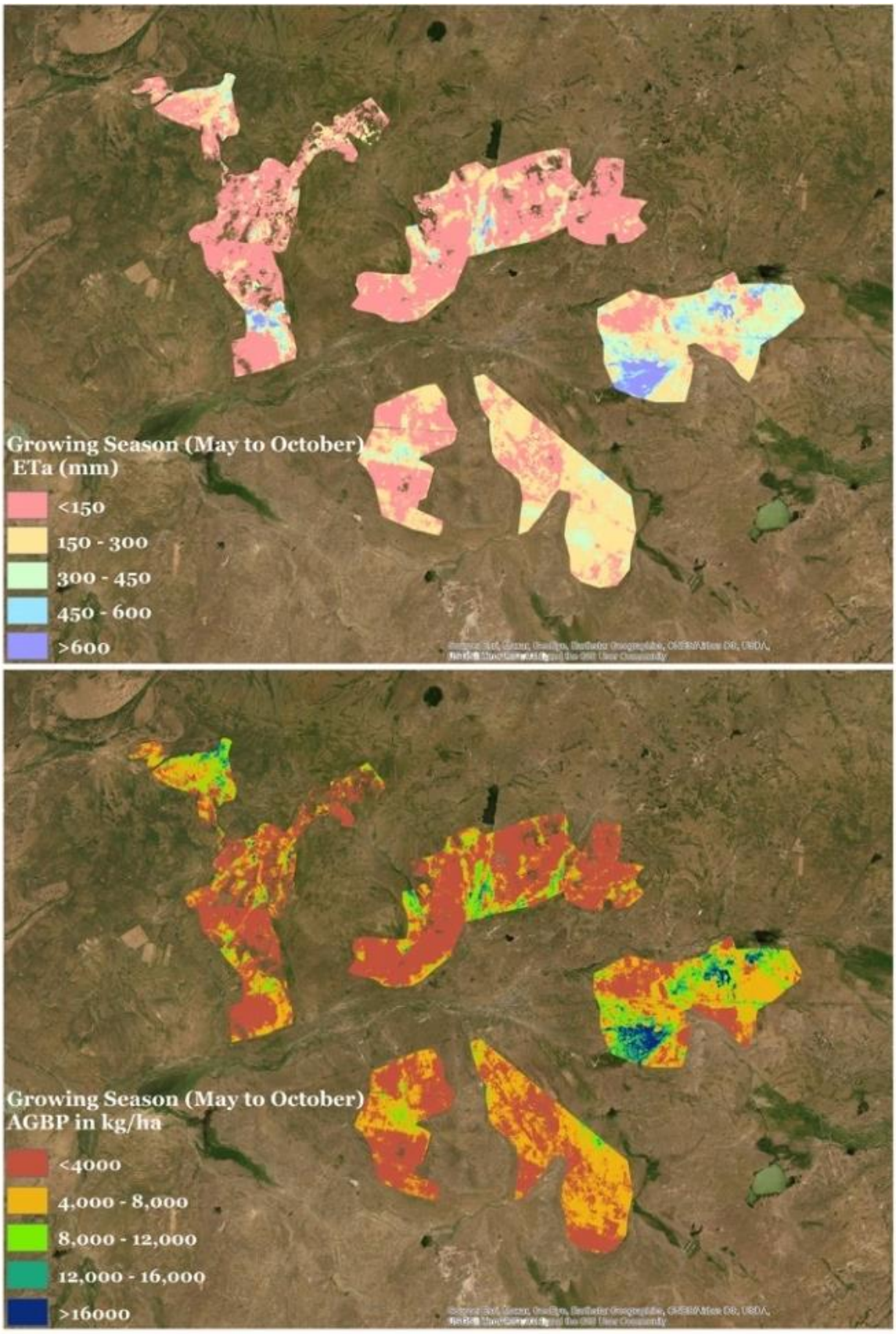

Figure 19: ET_a, RWD, AGBP and GBWP in the irrigated areas of Zhanaarka district in Karaghandy province

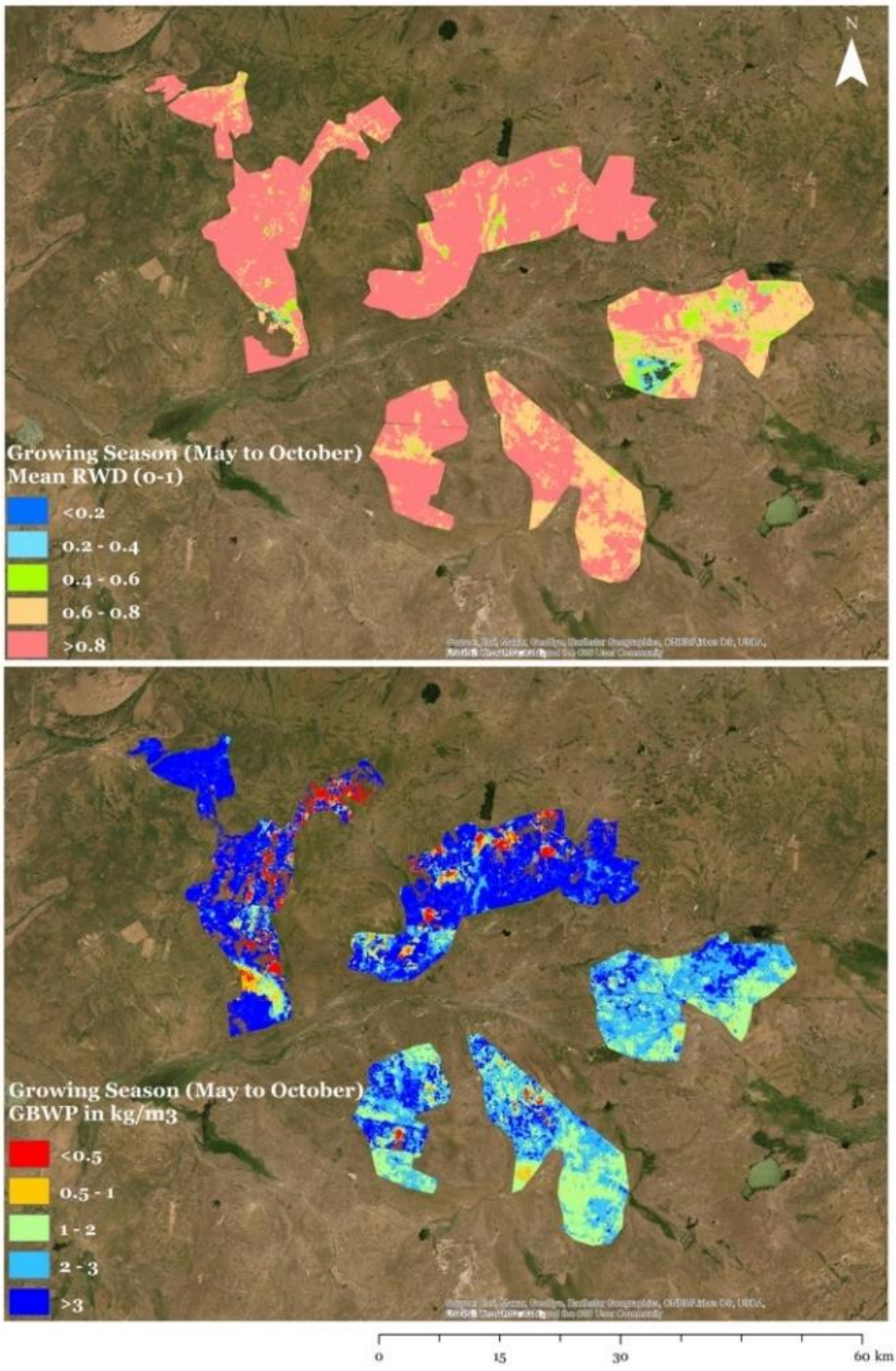

Figure 20: ET_a, RWD, AGBP and GBWP in the irrigated areas of Zhanaarka district in Karaghandy province

V. SUMMARY AND KEY FINDINGS

56. Given the vastness of the areas and the lack of available information on cropping systems and irrigation infrastructure, remote sensing data can provide a starting point to assess the current situation and to help prioritize areas for investment. The analysis presented here has focused on a remote sensing based assessment of water productivity and related parameters to characterize the spatial variability in agricultural water consumption and biomass production within the Karaghandy province. The study has focused on the identifiable irrigated areas in the Abay, Bukhar, Nura, Osakarov and Zhanaarka districts. Many of these areas have low water consumption, high water deficits, and low AGBP during the irrigation season. Overall the results indicate that there is big potential to increase the productive use of water in these locations.

57. While the locations of the Subprojects are not available, the data presented in this report have been described and interpreted for the major, large blocks of irrigation visible in the satellite data. However, as the results have been produced for the districts within the Karaghandy province within which the Subprojects are located, once more details are available regarding their locations and scheme layouts and cropping systems the data can be interpreted for these specific irrigation schemes to further characterize potential issues related to water delivery within them, and to prioritize investments accordingly.

58. The mean seasonal ET_a for the irrigated areas in Osakarov, Abay and Bukhar was 297 mm, 278 mm and 239 mm respectively, which is low for wheat. Nura and Zhanaarka were even lower, with mean values of 211 mm and 218 mm respectively. The mean seasonal AGBP in the irrigated areas of Osakarov, Abay and Bukhar was 8,071 kg/ha, 8,037 kg/ha and 7,739 kg/ha respectively, which is also low for wheat. Nura and Zhanaarka demonstrated the lowest values of 7,010 and 4,468 kg/ha respectively, suggesting that a large portion of the irrigated areas was either left fallow or a crop with lower biomass production than wheat with was cultivated in 2019.

59. Overall, the irrigated areas in Zhanaarka and Nura demonstrate lower seasonal levels of water consumption as compared to the irrigated areas in Abay, Bukhar and Osakarov. Osakarov and Abay in particular demonstrated areas of higher ET_a (600 mm), which potentially indicates better functioning irrigation schemes. However, other than the Osakarov district, most of the higher ET_a values were found in the irrigated areas closer to water channels. Water deficits were highest in the Nura and Zhanaarka irrigated areas during the 2019 irrigation season.

60. The location of the Koksun Subproject in Abay district has been identified; the maps demonstrate a clear pattern of higher values of both ET_a and AGBP near the outlet of the reservoir and at the head section of the scheme. To the north of this a declining trend in ET_a and AGBP is evident; the western portion of the scheme furthest away from the reservoir is under performing in comparison to the southeast. In addition, there is a section in the middle of the scheme which demonstrates much lower values than the surrounding areas. This suggests that there is likely to be an issue with water delivery to this parcel.

61. The possible location of Subprojects in the Osakarovsk district have been identified; the assessment of ET_a and AGBP values for these irrigation schemes, and the spatial patterns which are displayed suggests that there are dysfunctional water delivery systems in the far east and far west of the site. The middle sections of the schemes which appear to be fed by the main canal demonstrate greater water availability and higher production.

VI. LIST OF REFERENCES

Bastiaanssen, W. G. (2000). SEBAL-based sensible and latent heat fluxes in the irrigated Gediz Basin, Turkey. *Journal of hydrology*, *229*(1-2), 87-100.

Bastiaanssen, W. G., & Chandrapala, L. (2003). Water balance variability across Sri Lanka for assessing agricultural and environmental water use. Agricultural water management, 58(2), 171-192.

Bastiaanssen, W. G., Menenti, M., Feddes, R. A., & Holtslag, A. A. M. (1998). A remote sensing surface energy balance algorithm for land (SEBAL). 1. Formulation. Journal of hydrology, 212, 198-212.

CACILM SLMIS, 2009: Final Report, RETA 6357: Central Asian Countries Initiative for Land Management Multicountry Partnership Framework Support Project, September 2009

GFSAD 2020, https://lpdaac.usgs.gov/documents/172/GFSAD1K_User_Guide_V1.pdf

GLDAS 2020, GLDAS v2.1; https://ldas.gsfc.nasa.gov/gldas

IEE 2019, KAZ: Initial Environmental Examination, Irrigation Rehabilitation Project, Karaghandy Province Subprojects, Project No. 50387-001, Report to ADB

IHE Delft and IWMI, 2020. Water Productivity and Water Accounting: Methodology Manual. Delft, The Netherlands.

Jaafar, H.H., Ahmad, F.A., 2020. Time series trends of Landsat-based ET using automated calibration in METRIC and SEBAL: The Bekaa Valley, Lebanon. Remote Sens. Environ., Time Series Analysis with High Spatial Resolution Imagery 238, 111034.

Karatayev, M., Rivotti, P., Mourão, Z. S., Konadu, D. D., Shah, N., & Clarke, M. (2017). The water-energy-food nexus in Kazakhstan: challenges and opportunities. Energy Procedia, 125, 63-70.

FAO 2020. Accessed at http://www.fao.org/3/x6905e/x6905e0c.htm on October 2020.

Nugent, J. (2018). Cloudy with a chance of “cirrus” science. Science Scope, 42(2), 26-28.

Neteler, M., 2010. Estimating Daily Land Surface Temperatures in Mountainous Environments by Reconstructed MODIS LST Data. Remote Sens. 2, 333–351.

Metz, M., Andreo, V., Neteler, M., 2017. A New Fully Gap-Free Time Series of Land Surface Temperature from MODIS LST Data. Remote Sens. 9, 1333.

VII. ANNEX A

Table 5: Available Landsat 8 images during the 2019 irrigation season

10	Path		Month	Acquisition Date (DD/MM/YY)	Cloud cover	Average Cloud Cover
025	154		May	06/05/2019 22/05/2019	0% 80%	36%
			June	07/06/2019 23/06/2019	65% 0%	
			July	09/07/2019 25/07/2019	5% 57%	
			August	10/08/2019 26/08/2019	3% 0%	
			September	11/09/2019 27/09/2019	81% 100%	
			October	13/10/2019 29/10/2019	23% 17%	
025	155		May	06/05/2019 22/05/2019	0% 88%	47%
			June	07/06/2019 23/06/2019	79% 6%	
			July	09/07/2019 25/07/2019	28% 32%	
			August	10/08/2019 26/08/2019	20% 0%	
			September	11/09/2019 27/09/2019	84% 100%	
			October	13/10/2019 29/10/2019	68% 52%	
025	156		May	04/05/2019 20/05/2019	2% 68%	38%
			June	05/06/2019 21/06/2019	73% 11%	
			July	07/07/2019 23/07/2019	0% 100%	
			August	08/08/2019 24/08/2019	1% 0%	
			September	09/09/2019 25/09/2019	82% 28%	
			October	11/10/2019 27/10/2019	90% 0%	
026	154		May	06/05/2019 22/05/2019	0% 77%	37%
			June	07/06/2019 23/06/2019	97% 6%	
			July	09/07/2019 25/07/2019	1% 17%	
			August	10/08/2019 26/08/2019	0% 0%	
			September	11/09/2019 27/09/2019	78% 100%	
			October	13/10/2019 29/10/2019	62% 4%	
026	155		May	13/05/2019	4%	35%

				29/05/2019	15%	
			June	14/06/2019 30/06/2019	75% 0%	
			July	16/07/2019	0%	
			August	01/08/2019 17/08/2019	79% 47%	
			September	02/09/2019 18/09/2019	52% 23%	
			October	04/10/2019 20/10/2019	0% 93%	
026	156		May	04/05/2019 20/05/2019	0% 44%	36%
			June	05/06/2019 21/06/2019	7% 78%	
			July	07/07/2019 23/07/2019	0% 100%	
			August	08/08/2019 24/08/2019	0% 0%	
			September	09/09/2019 25/09/2019	62% 1%	
			October	11/10/2019 27/10/2019	100% 35%	